Propagation of high-power partially coherent fibre laser beams in a real environment

Tao Ru-Mao(陶汝茂), Si Lei(司 磊), Ma Yan-Xing(马阎星), Zou Yong-Chao(邹永超), and Zhou Pu(周 朴)†

College of Optoelectric Science and Engineering, National University of Defense Technology, Changsha 410073, *China*

(Received 27 April 2011; revised manuscript received 10 May 2011)

The propagation performance of high-power partially coherent fibre laser beams in a real environment is investigated and the theoretical model of a high-power fibre laser propagating in a real environment is established. The influence of a collimating system and thermal blooming is considered together with atmospheric turbulence and mechanical jitter. The laser energy concentration of partially coherent beams in the far field is calculated and analysed based on the theoretical model. It is shown that the propagation performance of partially coherent beams depends on the collimating system, atmospheric turbulence, mechanical jitter and thermal blooming. The propagation performance of partially coherent beams and fully coherent beams is studied and the results show that partially coherent beams are less sensitive to the influence of thermal blooming, which results in that the energy degeneration for partially coherent beams is only 50% of that for fully coherent beams. Both partially coherent beams and fully coherent beams become less sensitive to thermal blooming when the average structural constant of the refraction index fluctuations increases to 1.7×10^{-14} $\mathrm{m}^{-2/3}$. The investigation presents a reference for applications of a high-power fibre laser system.

Keywords: fibre lasers, partially coherent beams, Gaussian–Schell mode beams, propagation

PACS: 42.55.Wd, 42.68.Ay, 42.68.Bz **DOI:** 10.1088/1674-1056/20/9/094208

1. Introduction

It is very important to study the propagation performance of laser beams in a real environment for a high-power fibre laser system. Much work has already been carried out and it has been shown both theoretically and experimentally that partially coherent beams are less affected by turbulence than fully coherent ones.[1−6] Fibre lasers have wide potential applications due to their essential characteristics such as high conversion efficiency, excellent beam quality, convenient heat management and compact configuration.[7,8] With the development of high-power laser diode pump technology and double-clad fibre production, the output power of fibre lasers is gradually increasing and the single-mode kilowatt fibre laser has become reality commercially.[9] However, the ultimate output power of a single fibre laser is limited due to the nonlinear effect, facet fracture and thermal lens.[10] If the requirement of the single mode is not needed, the output power can be increased significantly.[11] Therefore, study of high-power partially coherent fibre laser beams propagating in a real environment is of significant importance for the design and performance analysis of high-power fibre laser systems.

In this paper, taking the Gaussian–Schell mode (GSM) beam as a typical model, we analyse the propagation performance of partially coherent beams in a real environment and the influence of collimating systems, atmospheric turbulence, mechanical jitter and thermal blooming on the propagation efficiency of partially coherent beams, which is calculated numerically. The dependence of average power in the bucket (PIB) on propagation distance is obtained. Our investigation provides a good reference for the design of high-power fibre laser systems.

2. Theory analysis

The average intensity distribution of GSM beams has the same intensity distribution as Gaussian beams, which can be written as[9,12]

$$I = I_0 \frac{R_0^2}{R^2(z)} \exp\left[-\frac{2r^2}{R^2(z)}\right]. \tag{1}$$

The long-time averaged spot size at range z can

†Corresponding author. E-mail: zhoupu203@163.com

© 2011 Chinese Physical Society and IOP Publishing Ltd

be written as

$$R^2(z) = \left[R_0^2 + \theta_{\text{spread}}^2 z^2\right], \tag{2}$$

where R_0 is the initial value of the waist radius; and the spreading angle θ_{spread} contains contributions from the diffraction θ_{diff}. The beam quality contains the influence of beam collimating system θ_{quality}, atmospheric turbulence θ_{tur}, mechanical jitter θ_{jitter} and thermal blooming θ_{bloom}. For the purpose of discussion, we write the total spreading angle in the form of[9]

$$\theta_{\text{spread}}^2 = \left(\theta_{\text{diff}}^2 + \theta_{\text{quality}}^2 + \theta_{\text{turb}}^2 + \theta_{\text{jitter}}^2 + \theta_{\text{bloom}}^2\right). \tag{3}$$

This expression for the spreading angle is in excellent agreement with the more exact extended Huygens' principle formulation for describing the effects of turbulence and partial coherence.[9,12−15] The influence of the collimating system, atmospheric turbulence, thermal blooming and mechanical jitter on the total beam spreading angle will be discussed separately in the following subsections.

2.1. Influence of the collimating system

For a real high-power fibre laser system, laser beams first propagate through the collimating system before propagating in atmosphere and the beam degradation due to nonlinearities in transmissive optics may dominate atmospheric effects such as turbulence, among others.[16] To analyse and simulate the effects of geometrical and thermal aberrations in lenses on the optical beam quality of a high-power GSM beams by ray optics theory, we give the rays a transverse velocity distribution as[17,18]

$$g(\boldsymbol{v}_0) = (1/\pi\overline{v}^2)\exp(-|\boldsymbol{v}_0|^2/\overline{v}^2), \tag{4}$$

with the transverse velocity spread

$$\overline{v} = \lambda c/(\sqrt{2}\pi R_0\beta), \tag{5}$$

where $\boldsymbol{v}_0$ is the velocity and β is a space correlation parameter defined as

$$\beta = \left[1 + \left(\frac{R_0}{\sigma_0}\right)^2\right]^{-1/2}. \tag{6}$$

The optical beam quality parameter is expressed as[19]

$$M^2 = 1/\beta. \tag{7}$$

Then we can obtain

$$\theta_{\text{quality}}^2 = \left(\frac{\lambda}{\pi R_0}\right)^2 \left(M^4 - 1\right). \tag{8}$$

The beam quality M_i^2 after propagating through the ith lens is given by[18]

$$M_i^2 = \left[(M_{i-1}^2)^2 + \frac{\pi^2 R_{i0}^2}{2\lambda^2}\alpha_{i3}^2\right]^{1/2}. \tag{9}$$

For bi-concave or bi-convex lens,

$$\alpha_{i3} = \left[(n_{i0} - 1) + g_i\Delta T_i(0)\right]\left(\frac{R_{i0}^3}{R_{ic}^3}\right) + g_i\overline{T}_i\frac{4L_{i0}}{R_{i0}}\left(1 - \frac{2R_{i0}^2}{R_{ic}L_{i0}}\right), \tag{10a}$$

$$\Delta T_i(0) = \gamma(2R_{i\text{L}}^2/R_{i0}^2)\overline{T}_i, \tag{10b}$$

$$g_i = (\partial n/\partial T)_i + (n_{i0} - 1)\alpha_{iT}, \tag{10c}$$

$$\overline{T}_i \equiv \alpha_i p/(4\pi\kappa_i), \tag{10d}$$

where R_{i0}, R_{ic}, L_{i0} and n_{i0} stand for the spot size, the radius of curvature, the lens thickness on axis and the refractive index of the ith lens, respectively; λ is the wavelength of the laser beams, κ_i is the thermal conductivity, α_i is the absorption coefficient, $p = \left(\pi R_{i0}^2 I_0\right)/2$ is the beam power; and $\gamma(x) = \gamma_0 + \Gamma(0, x) + \ln(x)$, $\gamma_0 \approx 0.58$. In a uniform medium, the spot size is given by

$$R^2(z) = R_0^2\left(1 - \frac{z}{L_{\text{f}}}\right)^2 + \left(M^2\theta_0 z\right)^2, \tag{11}$$

where L_{f} is a constant that determines the focal length and $\theta_0 = \lambda/\pi R_0$ is the diffraction angle of a Gaussian beam.

2.2. Influence of atmospheric turbulence

The influence of the atmospheric turbulence is mainly determined by the coherent length. Due to atmospheric turbulence, the laser spot will be extended and the spreading angle of GSM beams can be written as[12−15]

$$\theta_{\text{tur}}^2 = 2\cdot\left(\lambda/\left(\pi\rho_0\right)\right)^2, \tag{12}$$

where $\rho_0 = \left(0.545\bar{C}_n^2 k^2 L\right)^{-3/5}$ is the coherent length of spherical waves, $\bar{C}_n^2$ is the average structural constant of the refraction index fluctuations $C_n^2(h)$ that determines the strength of the turbulence and is a function of altitude h.[20,21] $\bar{C}_n^2$ can be calculated by using

$$\bar{C}_n^2 = \frac{\sec\zeta}{H}\int_0^H C_n^2(h)\,\mathrm{d}h, \tag{13}$$

where ζ is the zenith angle.[22]

To model the structural constant of the turbulence we use the Hufnagel–Valley $C_n^2(h)$ model[22]

$$C_n^2(h) = 5.94\times10^{-53}\left(\frac{21}{27}\right)^2 h^{10}\exp\left(-\frac{h}{10^3}\right) + 2.7\times10^{-16}\exp\left(-\frac{h}{1.5\times10^3}\right) + 1.7\times10^{-14}\exp\left(-\frac{h}{10^2}\right). \quad (14)$$

2.3. Influence of thermal blooming

High-power laser beams propagating in atmosphere will induce thermal blooming owing to the self-induced spreading, distortion and bending of a laser beam, which occurs as a result of the absorption of a small fraction of the laser power by molecular and aerosol constituents in the atmosphere. Thermal blooming can limit the maximum irradiance that would propagate to a target regardless of the available transmitter power.[23−27] Considering the absorption, Eq. (1) can be rewritten as [23,25,26]

$$I = I_0\frac{R_0^2}{R^2(z)}\exp\left[-\frac{2r^2}{R^2(z)}-\alpha_{\rm atm}z\right], \quad (15)$$

where $\alpha_{\rm atm}$ is the absorption coefficient.

The expression for $p_{\rm t}$, the total beam power at threshold for the onset of thermal blooming in a transverse flow, is written as[24]

$$p_{\rm t}\simeq\frac{\pi}{4}\frac{\gamma P_0}{\gamma-1}\frac{1}{\alpha_{\rm atm}(n_{0\rm atm}-1)}\frac{\lambda^2 v}{R}, \quad (16)$$

where γ is the ratio of the molar specific heat C_P to C_V at constant pressure and volume, v is the wind velocity and R is the beam radius.

For the case of a collimated beam with a uniform wind velocity v in the x-direction, the strength of the thermal blooming is conveniently expressed in terms of the parameter N, which for a collimated beam can be written as[25−27]

$$N_{\rm c} = \left(\frac{-2\,({\rm d}n/{\rm d}T)\,I_0 z}{n_{0\rm atm}\rho C_P v R_0}\times\left[1-\frac{(1-{\rm e}^{\alpha_{\rm atm}z})}{\alpha_{\rm atm}z}\right]\right), \quad (17)$$

where $n_{0\rm atm}$, ${\rm d}n/{\rm d}T$ and ρ are, respectively, the refractive index, index change with respect to temperature and density.

To account for the small divergence of the beam, N must be multiplied by the ratio $(R_0/R(z))$[26,28,29]

$$N = N_{\rm c}\left(\frac{R_0}{R(z)}\right) = \left(\frac{-2\,({\rm d}n/{\rm d}T)\,I_0 z}{n_{0\rm atm}\rho C_P v R_0}\times\left[1-\frac{(1-{\rm e}^{\alpha_{\rm atm}z})}{\alpha_{\rm atm}z}\right]\right)\left(\frac{R_0}{R(z)}\right), \quad (18)$$

where R_0 and $R(z)$ are the initial and final beam radii if blooming is not present. The laser spreading angle of GSM beams due to thermal blooming can be written as[30,31]

$$\theta_{\rm bloom}^2 = \left(\frac{\lambda}{\pi R_0}\right)^2\left(0.0625N^2\right). \quad (19)$$

2.4. Influence of mechanical jitter

In a real transmitting system, mechanical jitter is inevitable, especially in the optical tracking system. Due to the tracking jitter induced by the residual tracking errors, the laser beams will wander and extend, resulting in a decrease of the laser energy concentrating on the target surface. The spreading angle of GSM beams due to mechanical jitter can be written as[32]

$$\theta_{\rm jitter}^2 = (1.57\sigma_{\rm jitter})^2, \quad (20)$$

where $\sigma_{\rm jitter}$ is the root-mean square (RMS) value of the jitter angle.

2.5. Analysis of the combined influence

For the applications such as energy transmission, the power in a certain area is a key parameter to our concern. Take the influence of the above factors into consideration, the PIB in the far field is given by

$$p_{\rm PIB} = p\times\frac{\int_{-a}^{a}\int_{-a}^{a} I\,{\rm d}x\,{\rm d}y}{\int_{-\infty}^{\infty}\int_{-\infty}^{\infty} I\,{\rm d}x\,{\rm d}y}, \quad (21)$$

where we consider the PIB with radius a.

3. Numerical calculations

The configuration of the collimating system is shown in Fig. 1 (the right dashed frame) and the structural parameters are listed in Table 1. The collimating system is a confocal telescope containing two bi-convex lenses. The value of $R_{2\rm c}$ is variable and different values stand for different collimating systems.

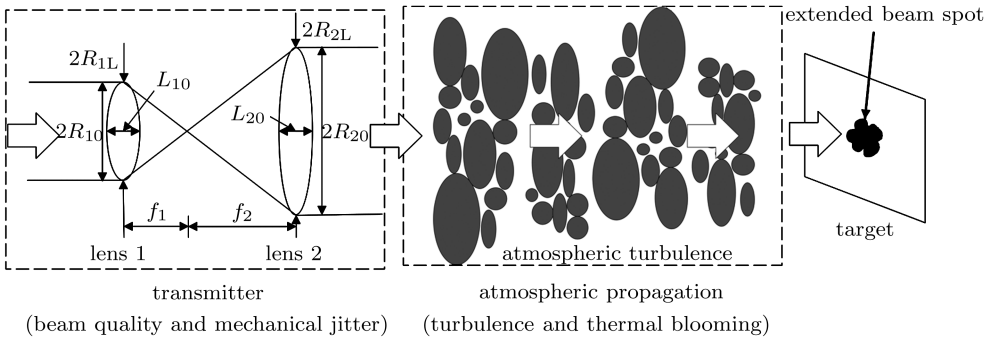


Fig. 1. Schematic diagram of partially coherent beams propagating in a real environment.

The value of $R_{2\mathrm{L}}$ changes as[18]

$$R_{2\mathrm{L}} = (3/4)R_{2\mathrm{c}}\left[1-\left(1-\frac{L_{20}}{2R_{2\mathrm{c}}}\right)^2\right]^{1/2}. \quad (22)$$

The thermal and optical parameters for the materials used in our model are summarized in Table 2.[17]

Table 1. Structural parameters of the collimating system.

Structural parameter	Lens 1	Lens 2
R_{L}/mm	3.00	40.00
L_0/mm	2.20	7.00
R_{c}/mm	−10.65	variable quantity
f/mm	9.00	500.00

Table 2. Thermal and optical parameters for UV-grade fused silica.

Parameter	Value
α/ cm^{-1}	5×10^{-5}
κ/ W · cm^{-1} · K^{-1}	1.4×10^{-2}
$(\partial n/\partial T)$/K^{-1}	10^{-5}
$\alpha_T = L^{-1}(\partial L/\partial T)$/K^{-1}	5.1×10^{-7}
ρ_0/ g · cm^{-3}	2.2
C_P/ J · g^{-1} · K^{-1}	0.75

Assume $\zeta = 45°$, the RMS mechanical jitter angle $\sigma_{\mathrm{jitter}} = 2.5$ μrad, $\lambda = 1$ μm, $R_0 = 0.5$ mm,[9] $\sigma_0 = 0.25$ mm, $p = 10$ kW and $a = 5.6$ cm. From Eqs. (1) and (21), we can obtain the dependence of average PIB on propagation distance for different collimating systems, as shown in Fig. 2. When $|R_{2\mathrm{c}}|$ is smaller than 1000 mm, the average PIB at certain distance increases with the increase in $|R_{2\mathrm{c}}|$. When $|R_{2\mathrm{c}}|$ is equal to 1000 mm, the average PIB stays the same unless the propagation distance is further than 1 km. The average PIB at a certain distance decreases with the increase in $|R_{2\mathrm{c}}|$ when $|R_{2\mathrm{c}}|$ becomes larger than 1000 mm. To achieve the best far-field PIB, a properly designed collimating system is indispensable, for example, $|R_{2\mathrm{c}}| = 1000$ mm for the system described above.

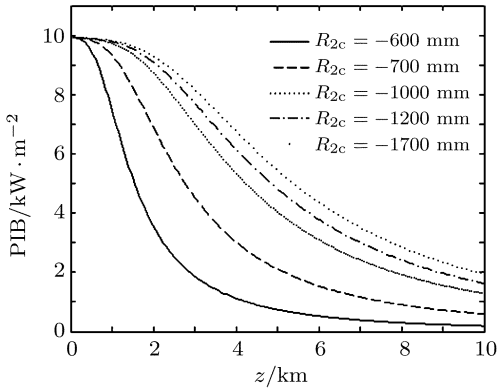


Fig. 2. Dependence of PIB on the propagation distance for different collimating systems.

Assume $|R_{2\mathrm{c}}| = 1000$ mm and the other parameters are taken to be the same as those in Fig. 2. The dependence of the average PIB on propagation distance under different zenith angles is presented in Fig. 3. If the partially coherent beam propagates along the horizontal direction, the PIB will decrease rapidly when the range is larger than 500 m. When it propagates with a certain zenith angle, the range in which the PIB stays the same increases to 1 km and the average PIB is improved dramatically. When the propagation distance is larger than 1 km, the decreasing speed of the PIB is evidently slower than that in the horizontal direction.

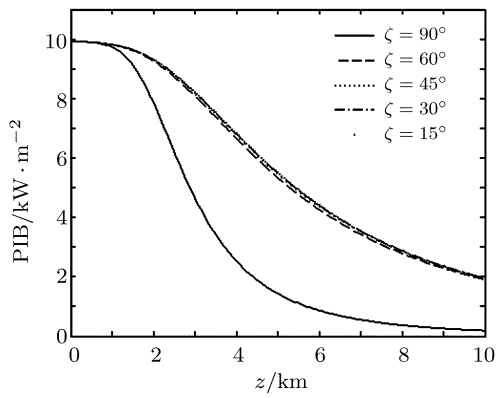


Fig. 3. Dependence of PIB on propagation distance for different zenith angles.

Assuming that $\zeta = 45°$, $|R_{2c}| = 1000$ mm, and the other parameters stay the same, we can obtain the dependence of the average PIB on the propagation distance with different jitter errors, as shown in Fig. 4. From Fig. 4, we see that the PIB is insensitive to mechanical jitter when the propagation distance is small, for example, less than 1 km. With the increase of propagation distance, the effects of mechanical jitter become evident. When $\sigma_{\rm jitter} = 5$ μrad, the average PIB is only 87.5% of the value when $\sigma_{\rm jitter} = 1$ μrad at distance 5 km; and when $\sigma_{\rm jitter} = 5$ μrad, the value decreases to 62.5%.

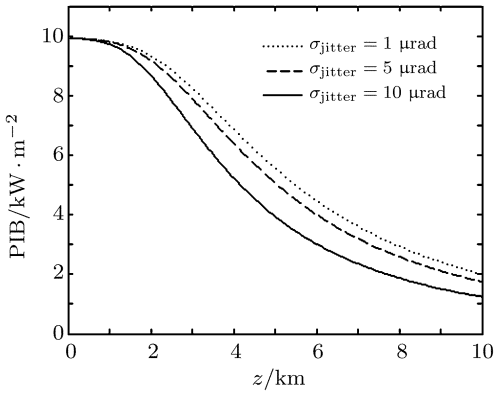


Fig. 4. Dependence of PIB on propagation distance with different jittering angles.

In the above discussion, the effects of thermal blooming are not considered. According to Eq. (16), taking the typical values of $P_0 = 10^5$ N · m^{-2}, $n_0 - 1 = 3 \times 10^{-4}$, $\gamma = 1.4$, $\alpha_{\rm atm} = 0.012$ km^{-1},[24] $R = 4$ cm, $v = 2$ m/s, we can obtain $p_{\rm t} \simeq 8$ kW as the threshold level for thermal blooming in air. So the effects of the thermal blooming must be taken into consideration. The dependence of the average PIB on propagation distance is presented in Fig. 5, using Eqs. (15), (19) and (21) (the parameters are taken to be the same as that in Fig. 4). The average PIB at $z = 5$ km for $v = 4$ m/s is 68.2% of that value for $v = 10$ m/s, and the value for $v = 1$ m/s decreases to only 10%. The transverse wind can mitigate the effects of thermal blooming and the effects of thermal blooming can be ignored when $v > 10$ m/s.

We also calculate the dependence of average PIB on propagation distance, with and without thermal blooming under different atmospheric turbulence intensities for partially coherent beams and fully coherent beams ($M^2 = 1$) (the parameters are the same as that in Fig. 5 except $v = 3$ m/s). The results are shown in Fig. 6. From Fig. 6(a), the difference between the PIB with blooming and that without blooming for partially coherent beams is about 50% of that for fully coherent beams, and we can conclude that partially coherent beams are less sensitive to the influence of thermal blooming than fully coherent beams.

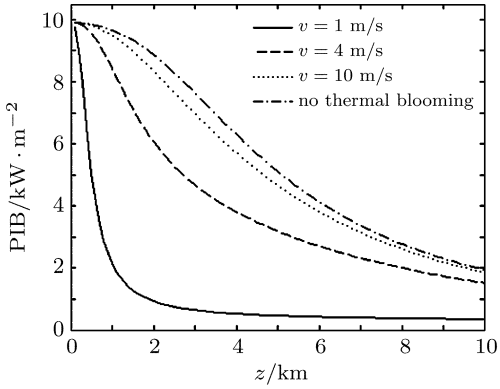


Fig. 5. Dependence of the PIB on propagation distance for different cross wind velocities.

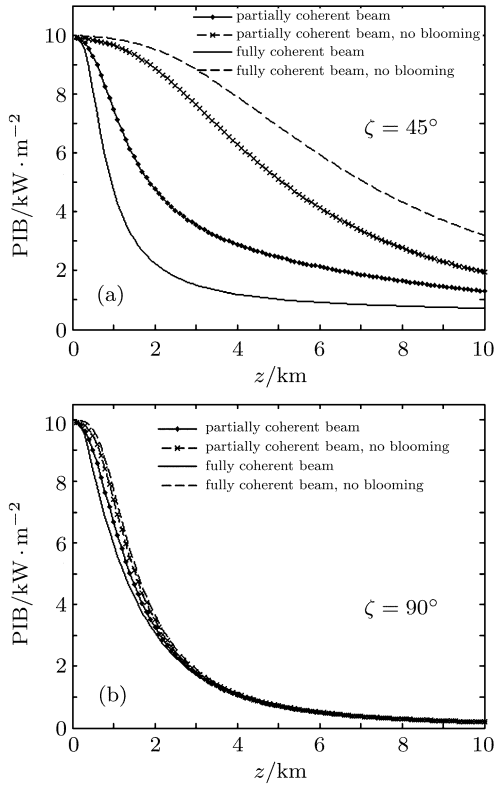


Fig. 6. Dependence of the PIB on propagation distance for different beam types. (a) The propagation of laser beams in a slanted path and $\overline{C}_n^2 = 4.3 \times 10^{-16}$ m$^{-2/3}$ in the range $z = 10$ km, (b) the propagation of laser beams in the horizonal direction, $\overline{C}_n^2 = 1.7 \times 10^{-14}$ $m^{-2/3}$ in the range $z = 10$ km.

This can be understood easily, for partially coherent beams have a stronger diffraction effect, which will counteract the thermal blooming.[28,29] Comparing the results of Figs. 6(a) and 6(b), we see that the influence of thermal blooming on both partially coherent beams and fully coherent beams becomes negligibly small when $\overline{C}_n^2$ is increased to 1.7×10^{-14} m$^{-2/3}$,

which corresponds to stronger turbulence effects; and we can obtain that the effects of atmospheric turbulence can counteract the effects of thermal blooming due to the much stronger influence of the atmospheric spreading effects that may counteract or limit the thermal self-focusing tendency.

4. Conclusions

We have presented a series of numerical simulations intended to evaluate the influence of a real environment on the propagation performance of partially coherent beams. It was shown that this performance depends on the influence of system design and atmospheric condition:

1) The design of collimating systems affects considerably the far-field energy concentration and a best far-field energy concentration can be acquired through optimizing the collimating system.

2) The propagation performance also depends on atmospheric turbulence and the far-field energy concentration will be improved dramatically when propagating along a certain pitching angle.

3) The stability of the platform also impacts the performance and the tracking, thus mechanical jitter should be mitigated to achieve a better performance.

4) Compared with fully coherent beams, partially coherent beams are less sensitive to thermal blooming.

5) Atmospheric turbulence can suppress the influence of thermal blooming.

The calculations in this paper are based on a simplified model and a more accurate analysis based on the pure numerical simulation is under study.

References

[1] Ji X L and Pu Z 2008 *Appl. Phys.* B **93** 915

[2] Cai Y J and Qiang L 2007 *Optik* **120** 146

[3] Zhu Y B, Zhao D M and Du X Y 2008 *Opt. Express* **16** 18437

[4] Wu J 1990 *J. Mod. Opt.* **37** 671

[5] Zhang E T, Ji X L and Lü B D 2009 *Chin. Phys.* B **18** 571

[6] Xiao R, Hou J and Jiang Z F 2008 *Acta Phys. Sin.* **57** 853 (in Chinese)

[7] Richardson D J, Nilsson J and Clarkson W A 2010 *J. Opt. Soc. Am.* B **27** B63

[8] Wang X L, Zhou P, Ma Y X, Ma H T, Xu X J, Liu Z J and Zhao Y J 2010 *Acta Phys. Sin.* **59** 5474 (in Chinese)

[9] Sprangle P, Ting A, Penano J, Fischer R and Hafizi B 2009 *IEEE J. Quantum Electronics* **45** 138

[10] Leger J R, Nilsson J, Huignard J P, Napartovich A P and Shay T M 2009 *IEEE J. Sel. Top. Quantum Electron* **15** 237

[11] Liu Z J, Zhou P and Xu X J 2008 *High Power Laser and Particle Beams* **20** 1795 (in Chinese)

[12] Ji X L and Ji G M 2008 *J. Opt. Soc. Am.* A **25** 1246

[13] Shirai T, Dogariu A and Wolf E 2003 *Opt. Lett.* **28** 610

[14] Dan Y Q, Zeng S G, Hao B Y and Zhang B 2010 *J. Opt. Soc. Am.* A **27** 426

[15] Wu G H, Guo H, Yu S and Luo B 2010 *Opt. Lett.* **35** 715

[16] Andrew L C and Phillips R L 2005 *Laser Beam Propagation through Random Media* (Washington: Press of SPIE) p. 395

[17] Penano J, Sprangle P, Ting A, Fischer R, Hafizi B and Serafim P 2009 *J. Opt. Soc. Am.* B **26** 503

[18] Tao R M, Si L, Ma Y X, Zou Y C and Zhou P 2011 *Acta Phys. Sin.* (Accepted)

[19] Palma C and Cincotti G 1997 *J. Opt. Soc. Am.* A **14** 1885

[20] Chu X X, Liu Z J and Wu Y 2008 *J. Opt. Soc. Am.* A **25** 7479

[21] Cai Y, Chen Y, Eyyuboglu H T and Baykal Y 2007 *App. Phy.* B **88** 467

[22] Piatrou P and Roggemann M 2007 *Appl. Opt.* **46** 6831

[23] Gebhardt F G 1976 *Appl. Opt.* **15** 1479

[24] Walsh J L and Ulrich P B 1978 *Laser Beam Propagation in the Atmosphere: Thermal Blooming in the Atmosphere* (New York: Springer-Verlag) pp. 226–227

[25] Gebhardt F G and Smith D C 1971 *IEEE J. Quantum Electronics* **7** 63

[26] Smith D C 1977 *Proc. IEEE* **65** 1679

[27] Gebhardt F G 1990 *Proc. SPIE* **1221** 1

[28] Gebhardt F G and Smith D C 1972 *Appl. Opt.* **11** 244

[29] Schoen N C and Novoseller D E 1983 *Appl. Opt.* **22** 3366

[30] Rao R Z 2006 *Infrared and Laser Engineering* **35** 130 (in Chinese)

[31] Huang Y B and Wang Y J 2004 *Proc. SPIE* **5639** 65

[32] Huang Y B and Wang Y J 2005 *Acta Opt. Sin.* **25** 152 (in Chinese)